ELSEVIER

Catalysis Today 70 (2001) 183–196

CATALYSIS TODAY

www.elsevier.com/locate/cattod

Study of the formation of $LaMO_3$ (M = Co, Mn) perovskites by propionates precursors: application to the catalytic destruction of chlorinated VOCs

G. Sinquin, C. Petit*, J.P. Hindermann, A. Kiennemann

Ecole Européenne de Chimie, Polymères et Matériaux de Strasbourg, Laboratoire d'Etude de la Réactivité Catalytique des Surfaces et Interfaces, UMR CNRS 7515, 25 rue Becquerel, 67087 Strasbourg Cedex 2, France

Abstract

$LaMO_3$ (M = Co, Mn) have been obtained by a sol–gel-like method with propionic acid as solvent. The influence of the nature of the metallic source (metal, nitrate or chloride) on the gel formation has been studied by fourier transform infrared spectroscopy (FTIR) and thermogravimetric analysis ATD–ATG. After calcination, the obtained perovskites have been characterised by X-ray diffraction (XRD), FTIR, X-ray photoelectron spectroscopy (XPS) and scanning electron microscopy (SEM) in order to investigate the influence of the preparation parameters on the final product. These mixed oxides have been used as catalyst for the destruction of chlorinated compounds. For each compound, the perovskite structure of $LaCoO_3$ decomposes in the same manner as LaOCl and Co_3O_4. Under the same test conditions, the perovskite with Mn is not altered. The stability of the structure has been explained by the formation of an oxygen overstoichiometric phase ($LaMnO_{3+\delta}$) which is thermodynamically more resistant to chlorination than the stoichiometric $LaMnO_3$. The catalytic behaviour of these oxides shows that two ways (hydrolysis and oxidation) are involved in the destruction of chlorinated hydrocarbons. The first one requires acidic sites and is less sensitive to the modification of the catalyst surface induced by chlorine than the second one requiring metallic oxidation sites.

Keywords: Perovskite; Stoichiometric phase; Volatile organic compound

1. Introduction

Volatile organic compounds (VOCs) are among the main pollutants in the low atmosphere of the cities and their release begins to be severely regulated [1]. Among the VOCs, the chlorinated compounds (CVOCs) represent about 16% of the worldwide release [2] and contribute efficiently to the destruction of the ozone layer in the stratosphere [3]. The decrease of CVOC release in air can be achieved in various ways: replacement of the chlorinated solvent by a non-chlorinated one, adsorption, condensation or incineration. Among the destructive processes the thermal incineration is actually the favoured method but requires high working temperatures which induce high energetic costs, formation of NO_x, dioxins and dibenzofurans [4]. Development of the catalytic oxidation of chlorinated VOCs is therefore of great interest. Two types of catalysts have been studied: supported noble metals [5,6] and oxides or mixtures of metal oxides [7–10]. The second one is, in general, less active than the first but more resistant to poisoning. However, they can lead to the formation of toxic volatile metallic chlorides or oxychlorides

* Corresponding author. Tel.: +33-388136976; fax: +33-388136975.
E-mail address: petitc@ecpm.u-strasbg.fr (C. Petit).

0920-5861/01/$ – see front matter
PII: S0920-5861(01)00417-5

as is the case with CrO_3 [11,12]. Mixed structures such as perovskites have the advantage of stabilising mixed-valence states of ions of useful transition metals and of being resistant to water and CO_2 even at high temperatures [13]. Results obtained in our laboratory [14–16] and by Kiessling et al. [17] have shown that rare earth perovskites present high potentials as catalysts for the destruction of chloromethanes, chloroethanes and chloroethenes.

The present paper concerns the control of the different steps of the formation of $LaMO_3$ (M = Co, Mn) perovskites in function of the nature of the initial metal precursor (metal, nitrate or chloride). The ageing of the structure under chlorinated gases is studied and compared with the observations of the structure formation with chlorinated salts. The difference in the stability of $LaCoO_3$ and $LaMnO_3$ in the presence of chlorine is discussed according to the thermodynamic data of the mixed oxides and the new phases observed after reaction with the chlorinated molecules.

2. Experimental

2.1. Perovskite synthesis

The synthesis of the $LaMO_3$ perovskites is based on the resin method from metallo-organic propionate precursors [18,19]. Lanthanum oxide was used (La_2O_3: 99.9% purity, Strem) as initial compound. Before use, the lanthanum oxide was calcined for 12 h at 900°C in order to decompose the easily formed lanthanum hydroxides, which would lead to a stoichiometry defect in the final perovskite. La_2O_3 was dissolved in an excess of hot propionic acid (140°C). This step requires about 1 h.

Three types of metallic sources were used to introduce the M element: nitrate salts $Co(NO_3)_2{\cdot}6H_2O$, $Mn(NO_3)_2{\cdot}4H_2O$; chloride salts $CoCl_2{\cdot}6H_2O$, $MnCl_2{\cdot}4H_2O$ and metallic Co, Mn. All the initial compounds have purity higher than 99%. The initial source of the M element was separately introduced in hot propionic acid until the formation of a limpid solution. The manganese and cobalt chlorides were not soluble in hot propionic acid. The solubilisation was obtained in that case after addition of a minimum amount of water. After dissolution, the two solutions were mixed and stirred under reflux for 1 h. Propionic acid was evaporated until formation of a resin, which hardened by cooling. In the presence of nitrate salts, nitrate species are eliminated as a reddish-brown nitrous oxide gas during the evaporation of propionic acid. For manganese, this step occurs almost at the end of evaporation of the solvent and is very exothermic. The obtained resins were calcined at 700°C for $LaCoO_3$ and 750°C for $LaMnO_3$ during 4 h (slope, 3°C/min) in order to obtain perovskite phases with the same order of crystallinity.

2.2. Techniques of characterisation

The X-ray diffraction (XRD) experiments were performed on a D5000 Siemens diffractometer using the Cu Kα radiation ($\lambda = 0.15406$ nm). The scattering intensities were measured over an angular range of $20^\circ < 2\theta < 85^\circ$ for all the samples with a step-size $\Delta(2\theta)$ of 0.03° and a count time of 2 s per step. The diffraction spectra have been indexed by comparison with the JCPDS files (joint committee on powder diffraction standards). The infrared spectra were recorded on an FTIR Nicolet 5DXC apparatus. The perovskite (3%) was mixed with KBr and pressed to form a disc of about 100 mg and 1 cm^2. Thermogravimetric analyses of the resin have been performed by TGA/TDA with a Setaram 92-1200 device. The gas flow consisted of a mixture of 10 ml min^{-1} of helium and 15 ml min^{-1} of air. The gases coming out of the balance were analysed by mass spectrometry. The XPS spectra were obtained with a VG (vacuum generator) ESCA 3 device at 10^{-8} Torr using Al Kα radiation ($h\nu = 1486.6$ eV). The spectra have been calibrated relatively to the C $1s_{1/2}$ binding energy of contamination carbon, which was fixed at 284.6 eV. The SEM analyses have been performed on a JEOL JSM-840 scanning microscope equipped with an EDX (energy disperse X-ray) device. A very thin carbon deposit was used to improve the conductivity of the sample. BET surface area have been determined using an SA 3100 coulter sorptometer at 77 K.

2.3. Reactor and operating conditions of tests

The activity of the catalysts was measured in a fixed bed reactor working at atmospheric pressure. A full description of the flow system which was used to measure the conversion and to detect the by-product

formation has already been described previously [14]. The ageing of the catalysts has been studied in the following conditions: 0.5 g catalyst (sieved between 0.125 and 0.250 mm), 3 l h^{-1} overall gas flow, 3.6% oxygen and 1.3% water in helium. The concentration of the chlorinated molecule was set to 2000 ppm of chlorine atoms (e.g. 1000 ppm for CH_2Cl_2 and 500 ppm for CCl_4).

3. Results

3.1. Characterisation of simple resins in function of the initial compound

To study the formation of the propionate gels, we started from La_2O_3 and from the transition element in the metallic state. The use of these compounds permits us to avoid the influence of other ligands such as NO_3^- and Cl^-. The dissolution of manganese in propionic acid was much faster than for cobalt. The formation of hydrogen has been observed during this step. The dissolution of the metal is thus obtained by oxidation of the metal by the propionic acid as given by the following equation:

$$2CH_3CH_2COOH + M^0 \rightarrow 2CH_3CH_2COO^- + M^{2+} + H_2 \quad (1)$$

The formation of the propionate precursors from La_2O_3 results from acid to basic reaction (2):

$$La_2O_3 + 6CH_3CH_2COOH \rightarrow 2La(CH_3CH_2COO)_3 + 3H_2O \quad (2)$$

The lower redox potential of manganese ($Mn^{2+}/Mn^0 = -1.1851$ V) compared with the cobalt ($Co^{2+}/Co^0 = -0.28$ V) explains the faster reaction of the former. The resins obtained after the evaporation of the excess of propionic acid are dried under vacuum, and then studied after dilution in KBr by FTIR. The main characteristic IR bands of the obtained resins of La and M element are given in Table 1 and compared with the bands of propionic acid. The band at 1717 cm^{-1} corresponds to the ν C=O vibration of free propionic acid. The bands near 1467 cm^{-1} (δ_{as} CH_3), near 1419 cm^{-1} (δ CH_2 scissors) and near 1380 cm^{-1} (δ_s CH_3) are common to all propionates and to propionic acid [20]. For La, Co and Mn, the propionate is bonded as bidentate propionate as shown by the band ν_{as} COO [21] located at 1549 cm^{-1} for the La and 1567 cm^{-1} for Co and Mn.

In the second step, the formation of manganese and cobalt propionates was studied by starting from nitrates. The dissolution from nitrates in propionic acid is very fast. During the evaporation of the solvent, a reddish-brown gas corresponding to NO_2 comes out of the solution. In the case of manganese this NO_2 departure occurs mostly at the end of evaporation and is very exothermic. This leads to the formation of a foam instead of a translucent gel as obtained by using the cobalt nitrates. The FTIR analysis of these foams showed the mixture of the precursors as propionates and nitrate species (ν NO_3 at 1384 cm^{-1} and π NO_3 at 825 cm^{-1}). A slow evaporation of the solvent leads progressively to the total nitrate departure and to the propionate formation. By this way, a translucent resin can also be obtained. The FTIR analysis of the gels is close to those obtained from metallic elements. Pure propionate precursors can thus also be obtained starting from nitrate salts.

The cobalt chloride and manganese chloride were not soluble in propionic acid under reflux. In both cases, the addition of a small amount of water permits dissolution of the salts. However, the obtained resins are opaque due to a back precipitation of the metallic chlorides when the added water was evaporated. The presence of metallic chloride in the resin has been

Table 1
FTIR characteristic bands (cm^{-1}) of propionate precursors obtained with La_2O_3 and metallic element (Mn, Co)

	ν C=O	ν_{as} COO bidentate	δ_{as} CH_3	δ CH_2 scissors	δ_s CH_3
Lanthanum	1716	1549	1469	1428	1376
Manganese	1716	1567	1467	1419	1377
Cobalt	–	1567	1467	1419	1377
Propionic acid	1717	–	1468	1417	1385

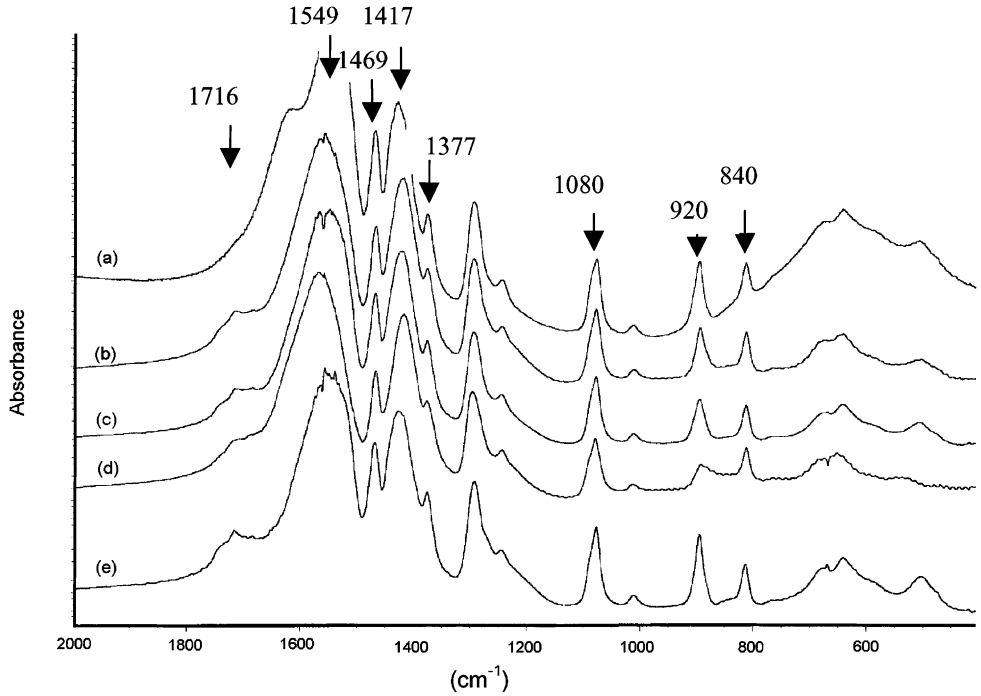

Fig. 1. FTIR spectra of: (a) precursors from $La_2O_3 + CoCl_2{\cdot}4H_2O$; (b) sum of the spectra (d) and (e); (c) precursors from $La_2O_3 + Co$; (d) precursors from Co^0; (e) precursors from La_2O_3.

confirmed by FTIR by the presence of additional bands at 1620 and 1628 cm^{-1} corresponding to the vibration of water present in $CoCl_2{\cdot}4H_2O$ and $MnCl_2{\cdot}4H_2O$, respectively. Unlike in the case of nitrates, the chlorides are not easily replaced by the propionates.

3.2. Characterisation of mixed resins in function of the initial compound

The FTIR spectrum corresponding to the mixed gel of La_2O_3 and M introduced in the metallic state (Co, Mn) were studied in comparison with the reference gels of the separate elements. The different FTIR spectra are given in Fig. 1 for cobalt. The results are similar with manganese. Spectra addition of the two individual resins can fit the spectra of the mixed resin. This indicates that no bridged La–Co or La–Mn propionate species are formed and the species remains in the bidentate form. The resin is formed by the condensation reactions between simple La and M propionates. The same observations are made with the resin obtained from the nitrate salts in the case of slow evaporation of the solvent. This result points out that the same propionate species are obtained in both cases.

The precursors obtained from La_2O_3 and the chlorinated salts were studied in the same manner by FTIR. From $CoCl_2{\cdot}4H_2O$, a new band at 1620 cm^{-1} is also observed and corresponds to the vibration δ(OH) of the water co-ordinated with H_2O from cobalt chloride (cf. Fig. 1a). Bidentate cobalt propionates are also observed but the ν_{as} COO vibration is shifted towards the lower frequencies: 1538 cm^{-1} (resin $La_2O_3 + CoCl_2{\cdot}4H_2O$) compared to 1551 cm^{-1} (resin $La_2O_3 + Co$). This can be correlated with the presence of chlorine ligands on Co in the propionate [19]. Same observations are made for the mixed resin obtained from $MnCl_2{\cdot}4H_2O$: a band of water at 1628 cm^{-1} and a shift of the ν_{as} COO vibration from 1555 to 1544 cm^{-1} by addition of chlorine. The use of chlorinated salts for M induces the presence of chlorine ligands, which are much more difficult to replace by propionates than nitrates.

A study of the mixed resin decomposition obtained from La_2O_3 + M salts by thermogravimetric and

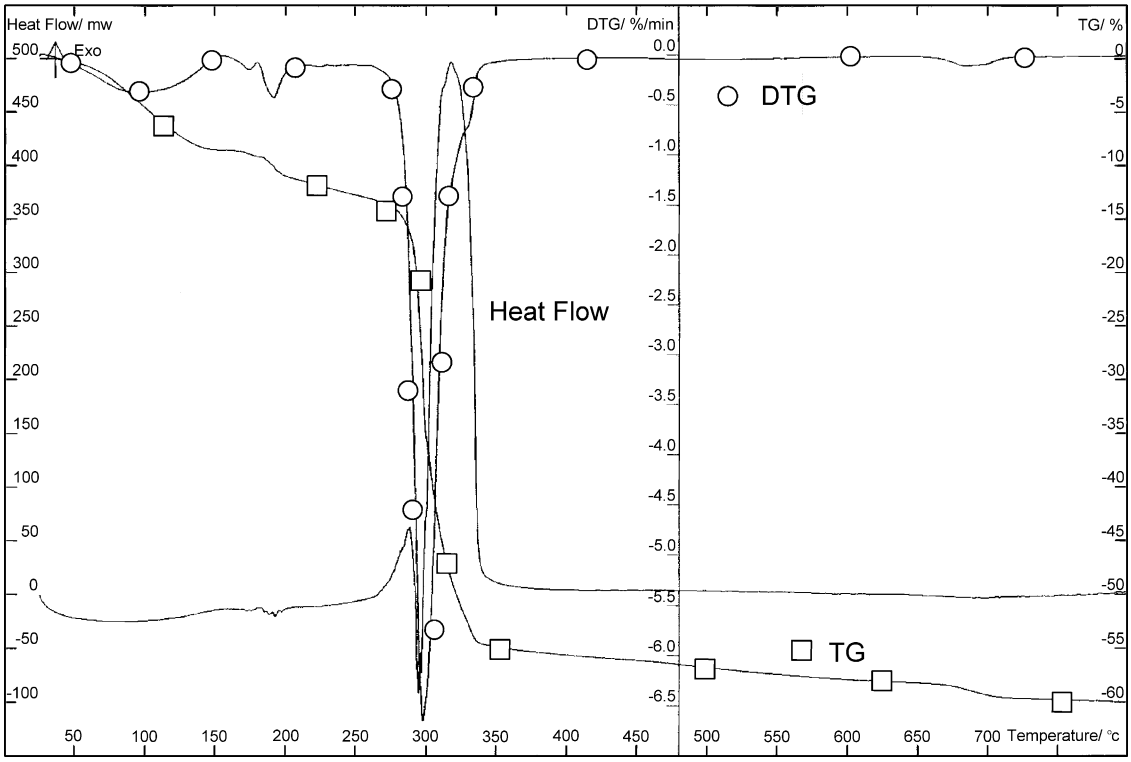

Fig. 2. TGA–DTA of the calcination of the gel obtained from $La_2O_3 + Mn$.

differential thermal analysis (TGA–DTA) has been made in function of the nature of the initial metal source. For metallic element (Co and Mn), the decomposition of the mixed gels are similar. The TGA–DTA analysis for $La_2O_3 + Mn$ is given in Fig. 2 as example.

The first weight loss corresponds to the evaporation of residual solvent (around 140°C). The main mass loss occurs around 300°C together with an endothermic peak. Pentan-3-one is detected by mass spectrometry at the same time. A part of the propionate ligand is thus decomposed by the Piria reaction and gave carbonate species as shown in the following equation:

$$M\text{–}(OOC\text{–}CH_2\text{–}CH_3)_2 \rightarrow CH_3CH_2COCH_2CH_3 + M\text{–}(CO_3) \quad (3)$$

The decomposition of the propionates is complete at 400°C and a high production of CO_2 and H_2O are observed. A very small weight loss occurs at 700°C and corresponds to lanthanum carbonates decomposition. The decomposition of the resins obtained with the nitrate salts presents a broadening of the exothermic peak, which keeps the same temperature position. The mass spectrometry analysis of the compound coming out of the thermobalance is given in Fig. 3 in the case of the mixed gel obtained with La_2O_3 and $Mn(NO_3)_2{\cdot}4H_2O$. NO or NO_2 have not been observed. This confirms the results previously obtained by FTIR showing that the nitrates are eliminated during the evaporation of propionic acid before the formation of resins.

The decomposition of the gels obtained with the metallic chloride presents an exothermic peak which is shifted above 350°C. Furthermore, a supplementary weight loss is observed around 750°C which is assumed to be due to the decomposition of lanthanum oxychloride.

We have shown in Table 2 the ratio between propionate and the sum of lanthanum and the metallic compounds by considering the total weight loss observed between 175 and 900°C. One observes that all the obtained ratio are below 2. By assuming that

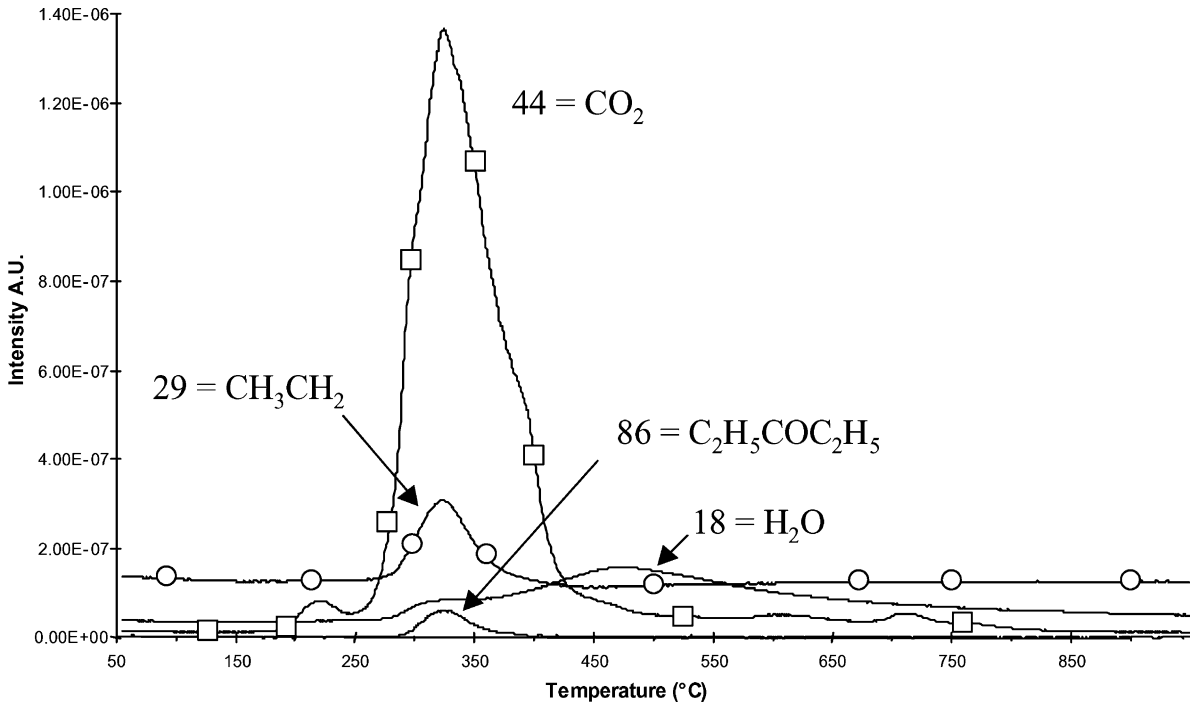

Fig. 3. Analysis of mass spectrometry of products obtained during the TGA–DTA from $La_2O_3 + Mn(NO_3)_2 \cdot 4H_2O$.

the transition metals are in +2 oxidation state, a value of 2.5 is required to fulfil the electroneutrality of the resins. As a consequence, we think that hydroxo (OH^-) or oxo (O^{2-}) are probably present in the propionate complexes. Indeed, various authors have already reported the formation of oxo-alcoxydes or oxo-carboxylates of different metals [22,23]. The presence of these oxo-bridges indicates an oligomerisation of the metallic complexes. In the case of tin propionates, Roger [24] has shown that the oligomeric chains remain relatively small (2.4 tin atoms per complex).

Table 2
Determination of the number of propionate ligands per metal atom

Sample	Ratio propionate/(La + M)
$La_2O_3 + Mn$ (s)	1.61
$La_2O_3 + Mn(NO_3)_2 \cdot 4H_2O$	1.56
Gel de $La_2O_3 + Co$ (s)	1.53
Gel de $La_2O_3 + Co(NO_3)_2 \cdot 6H_2O$	1.87

3.3. Characterisations (XRD, FTIR, XPS and SEM) of the perovskites

The precursors obtained from the mixed solution of metallic and nitrate salts of M being similar, the nature of the resulting perovskites should be the same as well. Indeed, no difference between the XRD patterns of the perovskites obtained from the metal or the nitrate salts has been observed. The only slight difference concerns the BET surface, a few higher for nitrate preparation than for metallic preparation. The phases obtained from chlorinated salts will be presented in the discussion part. None of the prepared $LaMO_3$ had the ideal cubic structure, but had a rhombohedric deformation, which can be indexed in the hexagonal system. The diffraction pattern obtained for $LaCoO_3$ corresponds to the stoichiometric perovskite described in the JCPDS file: 25-1060. The XRD data for lanthanum manganese oxide (calcined at 750°C) is nearer to the oxygen overstoichiometric structure $LaMnO_{3.15}$ referenced in the JCPDS 32-0484 file than to the stoichiometric $LaMnO_3$ perovskite (JCPDS 33-0713) which

Table 3
Characteristics of $LaMO_3$ (M = Co, Mn) obtained after calcination

	$LaCoO_3$[a]	$LaMnO_{3+\delta}$[a]
Calcination (°C)	700	750
Symmetry	Hexagonal	Hexagonal
Space group	D^6_{3d}	D^6_{3d}
Lattice parameters theoretical (Å)[b]		
$a = b$	5.441	5.523
c	13.088	13.324
Lattice parameters experimental (Å)		
$a = b$	5.421	5.466
c	13.090	13.461
Mean particle size (nm)	67	20
BET surface area ($m^2\,g^{-1}$)	9.2	17.1
Total pore volume ($cm^3\,g^{-1}$)	0.025	0.088

[a] Metallic nitrates have been used for the synthesis of the precursors.
[b] According to JCPDS files.

presents an orthorhombic symmetry. This overstoichiometric structure is often reported in literature on lanthanum manganese perovskite [25]. We have shown in Table 3 the calculated and theoretical lattice parameters of the two perovskites we have synthesised, their surface area and their total pore volume. The average mean particle size has also been calculated from the broadening of the peaks. It can be noted that $LaCoO_3$ presents a higher crystallinity than $LaMnO_{3+\delta}$. There is very good agreement between the experimental and reference lattice parameters for $LaCoO_3$, whereas the slight difference for $LaMnO_{3+\delta}$ is probably due to a difference in the oxygen over stoichiometry. Indeed the value of δ depends highly on the preparation conditions and has not been precisely measured.

The main FTIR bands were observed at 604 and 565 cm^{-1} for $LaMnO_{3+\delta}$ and at 598, 566, 424 cm^{-1} for $LaCoO_3$ after calcination. These band positions are in good agreement with the band of perovskite structures given in the literature [26] and confirm the data obtained by XRD analysis.

The scanning electron micrographs of $LaCoO_3$ and $LaMnO_{3+\delta}$ are shown in Figs. 4 and 5, respectively. The surface of $LaCoO_3$ presents a spongy appearance. At higher enlargement, this surface appears to be constituted by the aggregation of small particles (maximum size, 200 nm). EDX analysis leads to a Co/La ratio close to 1. For $LaMnO_{3+\delta}$, two different areas are observed. The first appears to be very dense and even at high magnification no crystallites are observed. The second is deposited like a crust of the first one and is formed by coils of about 2 μm diameter. The EDX analysis of the first domain gives a Mn/La ratio of 1, whereas the second is richer in manganese (59% Mn, 41% La). The analysis of the surface of these two perovskites has also been investigated by

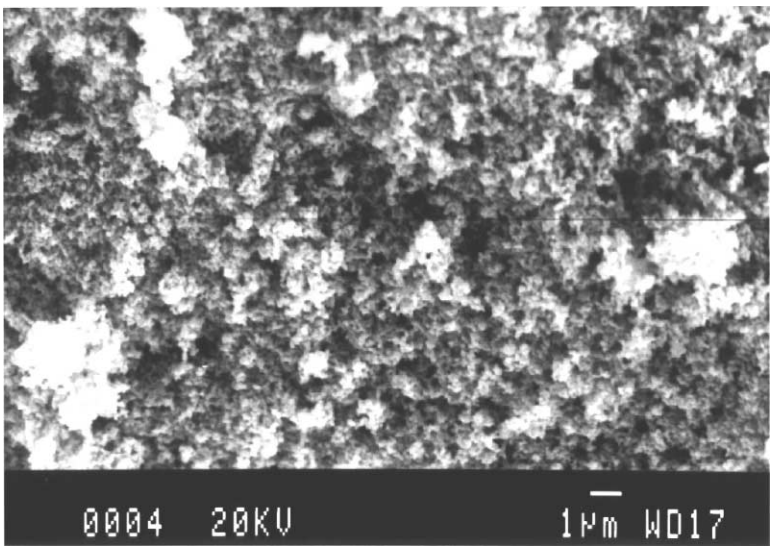

Fig. 4. Scanning electron micrograph for $LaCoO_3$.

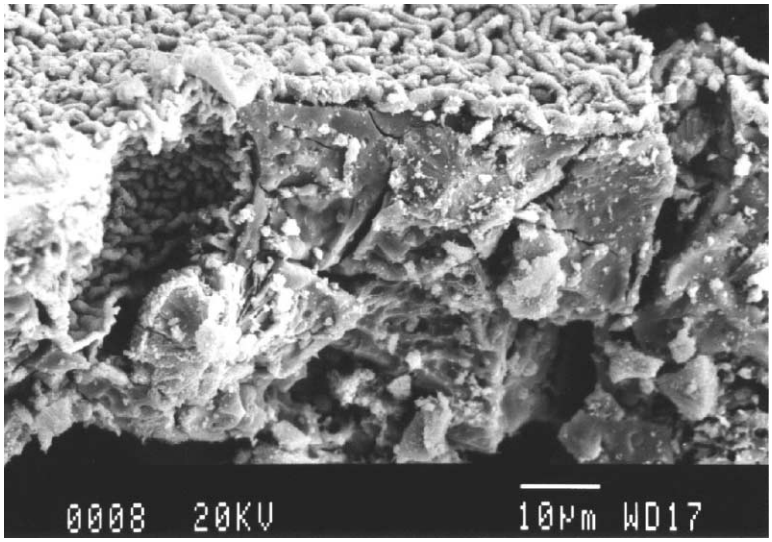

Fig. 5. Scanning electron micrograph for $LaMnO_{3+\delta}$.

XPS. The interpretation of the different energy levels (La $3d_{5/2}$, Mn $2p_{1/2}$ and Mn $2p_{3/2}$, Co $3p_{1/2}$ and Co $3p_{3/2}$) has already been discussed in detail in a previous paper [14]. We have shown that in both perovskites the majority of the metallic cations are in the +3 oxidation state. In the case of $LaCoO_3$, a characteristic satellite peak of Co^{2+} was observed at 789.9 eV [27]. However, its very low intensity indicates that the Co^{2+} is present only in low concentration. In the case of manganese, the absence of a satellite peak at +5 eV from the Mn $2p_{3/2}$ indicates that no Mn^{2+} is present. The presence of a slight amount of Mn^{4+} cannot be excluded and would agree with the oxygen overstoichiometric phase evidenced by XRD. Concerning the lanthanum, the signal at 833.9 eV observed for both structures was attributed to La^{3+} of the perovskite lattice. According to the literature, the peak observed at 835.7 eV observed on both perovskites was attributed to lanthanum carbonates [28]. The presence of carbonate species was confirmed by the presence of a peak at 289 eV in the C $1s_{1/2}$ signal [29,30]. The ratio M/La was calculated by taking into account the effective section of Co $2p_{3/2}$, Mn $2p_{3/2}$ and La $3d_{5/2}$ tabulated by Scofield [31]. We obtained $Co/La = 0.81$ for $LaCoO_3$ and $Mn/La = 0.46$ for $LaMnO_{3+\delta}$. There is thus a migration of the lanthanum towards the surface. This lanthanum, which is not incorporated in the perovskite structure, is present as lanthanum oxide whose one part is carbonated. Other authors have already observed this lanthanum excess on the perovskite surface. Tabata et al. [32] have, for instance, reported a Co/La of 0.81 in the case of $LaCoO_3$ obtained by using acetate precursors. Taguchi et al. [33] have shown that the La/Mn ratio can vary between 1.5 and 2 depending on the preparation parameters.

3.4. Ageing studies of the catalysts

The main results concerning the catalytic tests of the perovskites have been presented previously for C_1 [19] and C_2 [18] chlorinated compounds. We will focus here on the ageing studies performed under different chlorinated molecules. CH_2Cl_2 (1000 ppm) and CCl_4 (500 ppm) have been tested on $LaCoO_3$ and $LaMnO_{3+\delta}$. The temperature of the reaction has been set to give an initial conversion of 98%. The activity of $LaCoO_3$ and $LaMnO_{3+\delta}$ with CH_2Cl_2 and CCl_4 versus time are given in Figs. 6 and 7, respectively. With CH_2Cl_2, a deactivation occurs on $LaCoO_3$ (conversion shifts from 98 to 75% after 1 day on stream). The conversion is then stable at 75% for 175 h.

No noticeable deactivation has been observed on $LaCoO_3$ for CCl_4 and $LaMnO_{3+\delta}$ for the two tested chlorinated molecules. It must be noted that after 150 h under flow the catalysts have destroyed more than two times their own weight of chlorinated compound.

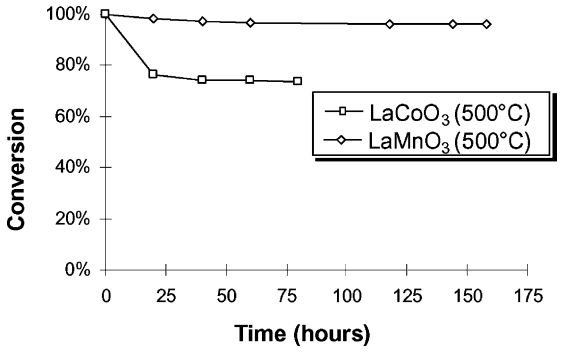

Fig. 6. Ageing test of $LaCoO_3$ and $LaMnO_{3+\delta}$ with 1000 ppm of CH_2Cl_2 ($T = 500°C$, 3.3% O_2, 1.3% H_2O).

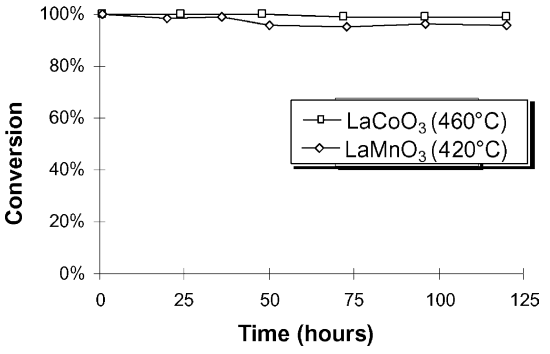

Fig. 7. Ageing test of $LaCoO_3$ ($T = 460°C$) and $LaMnO_{3+\delta}$ ($T = 420°C$) with 500 ppm of CCl_4, 3.3% O_2, 1.3% H_2O.

3.5. Characterisations after test

The evolution of the catalyst structure during the catalytic tests will be discussed in function of the nature of the perovskite and the nature of the chlorinated hydrocarbon used. Whatever may be the nature of tested chlorinated C_1 (presented here) or C_2 molecule (14), all FTIR spectra obtained after reaction on $LaCoO_3$ shows the formation of new bands at 665 and 574 cm^{-1} which can be attributed to Co_3O_4 and at 506–512 and 710 cm^{-1} (very weak) ascribed to LaOCl (Fig. 8). The XRD pattern obtained after reaction con-

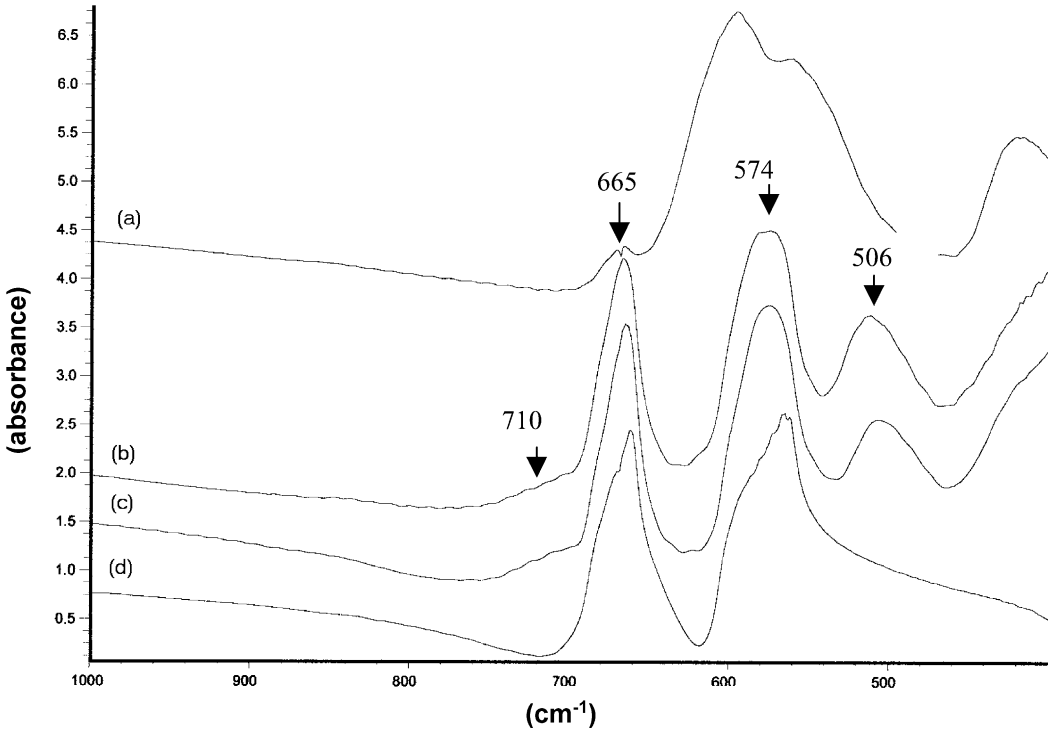

Fig. 8. FTIR spectra of: (a) $LaCoO_3$ before test; (b) $LaCoO_3$ after the ageing test with 1000 ppm of CH_2Cl_2 ($T = 500°C$, 3.3% O_2, 1.3% H_2O); (c) $LaCoO_3$ after the ageing test with 500 ppm of CCl_4 ($T = 460°C$, 3.3% O_2, 1.3% H_2O); (d) commercial Co_3O_4.

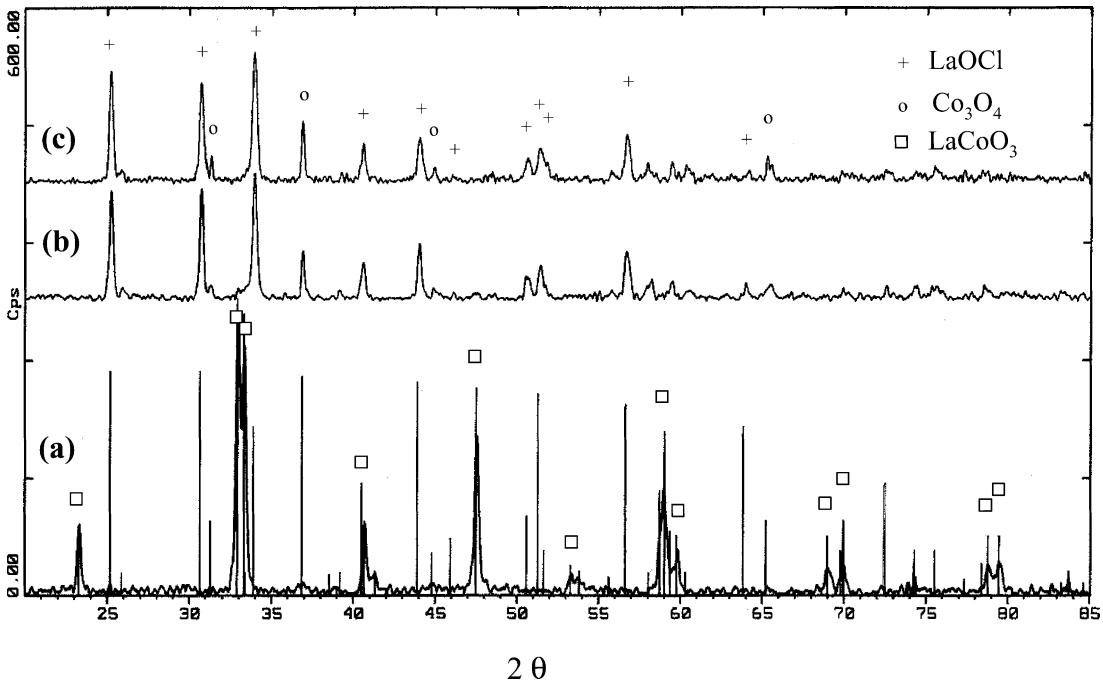

Fig. 9. XRD of $LaCoO_3$: (a) before test; (b) after the ageing test with 1000 ppm of CH_2Cl_2 ($T = 500°C$, 3.3% O_2, 1.3% H_2O); (c) after the ageing test with 500 ppm of CCl_4 ($T = 460°C$, 3.3% O_2, 1.3% H_2O).

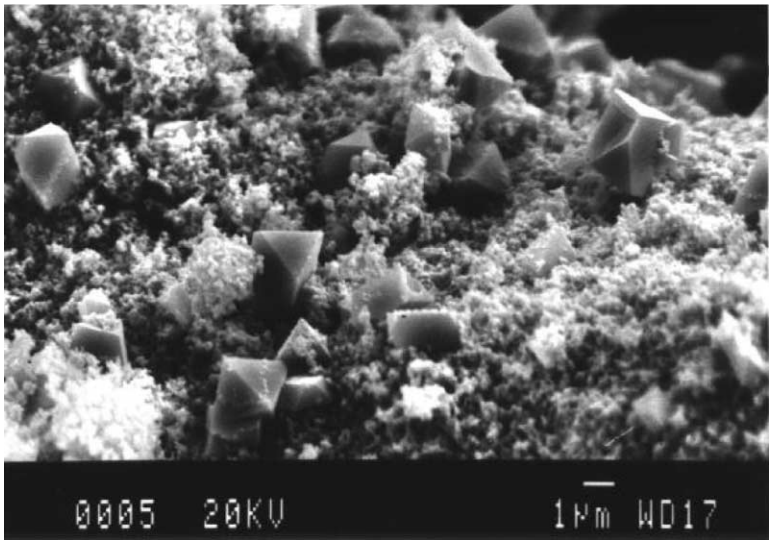

Fig. 10. Scanning electron micrograph for $LaCoO_3$ after the ageing test with 500 ppm of CCl_4 ($T = 460°C$, 3.3% O_2, 1.3% H_2O).

firms the destruction of the $LaCoO_3$ perovskite phase and the formation of LaOCl and Co_3O_4 (Fig. 9). The micrograph of $LaCoO_3$ after reactivity test is shown in Fig. 10. Octahedral crystallites of about 1–2 μm appears. The EDX analysis indicates that they essentially contain cobalt and can be considered as the Co_3O_4 phase observed by XRD. EDX analyses of the spongy part of the surface show that three elements are present (Co, La, Cl). The La/Cl ratio is always close to 1 and it is thus proposed that these parts correspond to LaOCl as suggested by FTIR and XRD. By XPS, no significant modification of the bonding energies of La 3d levels is observed on $LaCoO_3$ after reaction. The peaks of La linked to carbonates are still present. An important amount of chlorine has been observed after reaction on the catalyst surface. The $2p_{3/2}$ and $2p_{1/2}$ levels of chlorine are situated at about the same energies whatever the nature of the tested molecule (198 and 199.5 eV, respectively). These values are lower that the $2p_{1/2}$ binding energies observed for $CoCl_2$ at about 200.5 eV, but close to the $2p_{1/2}$ binding energies of LaOCl (199.7 eV). This indicates that chlorine atoms are preferentially linked to lanthanum. After reaction of CCl_4 or CH_2Cl_2 on $LaCoO_3$, the Co/La surface atomic ratio decreases drastically (0.1 and 0.04 compared to 0.81 before reaction). The formation of LaOCl and the sintering of the cobalt as big Co_3O_4 crystallites (observed by SEM) explain this huge decrease of the surface cobalt concentration. The migration of La to the surface is accelerated by the presence of chlorine in the gas phase, which induces the formation of LaOCl.

4. Discussion

The study of ageing under CH_2Cl_2 or CCl_4 has shown a large difference in the behaviour of catalyst stability. No deactivation of $LaCoO_3$ was observed with CCl_4 in spite of the structure loss. Contrarily, the behaviour of the catalyst with CH_2Cl_2 is very sensitive to the evolution of the structure. The evolution from $LaCoO_3$ to $LaOCl + Co_3O_4$ produces a decreasing of activity for CH_2Cl_2 but not a total deactivation. The mixture of LaOCl and Co_3O_4 is thus able to decompose CH_2Cl_2. We have already shown previously that hydrolysis and oxidation reactions both take part in the destruction of CH_2Cl_2 [19]. LaOCl is apparently a good catalyst for the hydrolysis of chlorinated C1 molecules. Indeed, La_2O_3 was almost inactive at 350°C to hydrolyse CCl_4 but the conversion increases with time when La_2O_3 was transformed into LaOCl. This result explains why no deactivation was observed during the decomposition of CCl_4, which can thus only proceed through hydrolysis on LaOCl. The deactivation observed in the case of CH_2Cl_2 points out that redox sites are required to destroy this compound.

FTIR or XRD shows no noticeable modification of $LaMnO_{3+\delta}$. The analysis of the catalyst surface by SEM after reaction does not show significant modifications. The coils are slightly altered (composition: 61% Mn, 35% La and 4% Cl instead of 59% Mn and 40% La). By XPS no significant modification of the bonding energies of La $3d_{5/2}$ and La $3d_{3/2}$ levels is observed on $LaMnO_{3+\delta}$ after reaction. A less important amount of chlorine has been observed after reaction on $LaMnO_{3+\delta}$. The $2p_{3/2}$ and $2p_{1/2}$ levels of chlorine are situated at about the same energies whatever the nature of the tested molecule (198 and 199.5 eV, respectively). These values are lower than the binding energies observed for $MnCl_2$ at about 199 eV, but close to the binding energies of LaOCl: Cl $2p_{3/2}$ (198.1 eV) and Cl $2p_{1/2}$ (199.7 eV). This indicates that chlorine atoms are preferentially linked to lanthanum like for $LaCoO_3$. If the Cl/(La + Mn) or Cl/(La + Co) ratio is considered, one obtains 1.36 for $LaMnO_{3+\delta}$ compared to 2.47 for $LaCoO_3$. This chlorine atoms are located only at the catalyst surface according to the EDX analysis of the aged $LaMnO_{3+\delta}$ giving an average Cl concentration much lower than for $LaCoO_3$. Furthermore, the manganese concentration at the catalyst surface is almost unchanged after reaction. This confirms that the surface of the lanthanum cobalt perovskite retains more chlorine than that of the lanthanum manganese perovskite, in agreement with the bulk analyses.

The evolution of the perovskite structure is in very good agreement with the results of the synthesis of the perovskites obtained by chlorides. From $CoCl_2{\cdot}4H_2O$ salt, the perovskite phase is not obtained after calcination at 700°C. A mixture of LaOCl and Co_3O_4 is observed with a similar XRD diffraction pattern as the $LaCoO_3$ samples obtained after reaction. In the case of $MnCl_2{\cdot}4H_2O$, the perovskite structure is formed (Fig. 11). A small formation of LaOCl is, however, observed on the diffractogram.

The stability of $LaMnO_{3+\delta}$ compared to $LaCoO_3$, which seems a priori surprising, can be explained

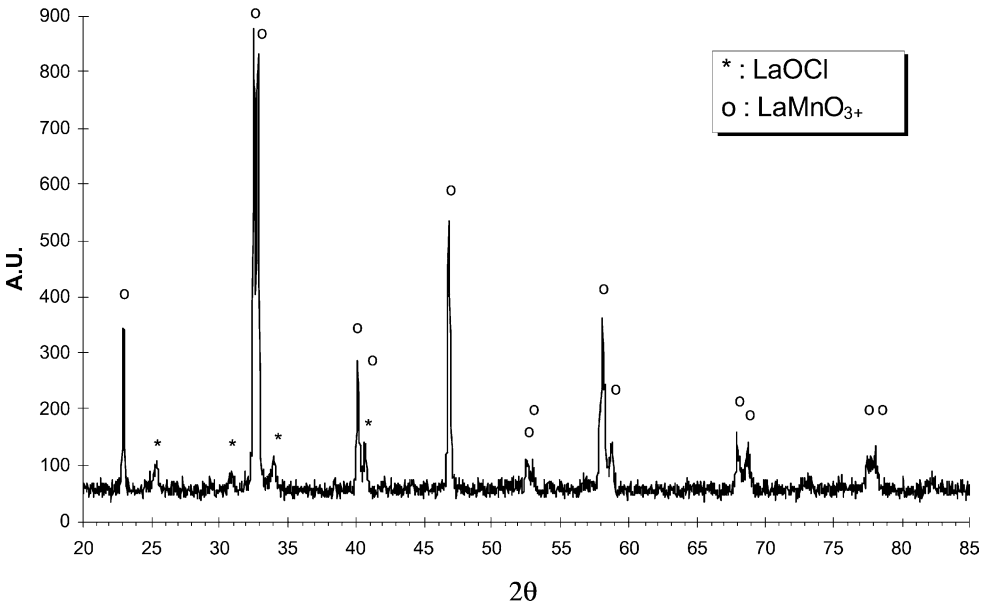

Fig. 11. XRD of the mixture from $CoCl_2 \cdot 4H_2O + La_2O_3$ in propionic acid after calcination at 750°C. References — LaOCl: JCPDS 34-1494, Co_3O_4: JCPDS 42-1467.

by thermodynamic considerations. The stabilisation enthalpy of the perovskite $\delta(LaMnO_3) = \Delta Gf^\circ(LaMO_3) - \frac{1}{2}\Delta Gf^\circ(La_2O_3) - \frac{1}{2}\Delta Gf^\circ(M_2O_3)$ can be computed by the relation proposed by Yokokawa et al. [34]. The following results are obtained for $LaCoO_3$ and $LaMnO_3$: $\delta(LaCoO_3) = -36\,kJ\,mol^{-1}$ and $\delta(LaMnO_3) = -43.9\,kJ\,mol^{-1}$. $LaCoO_3$ is, therefore, slightly less stable than $LaMnO_3$. However, our results indicate that the destruction of the perovskite structure is due to the formation of LaOCl in the presence of chlorinated molecules. The stability of the starting perovskites must thus be considered in the presence of chlorine and compared with the stability of the mixture of LaOCl and manganese or cobalt oxides as indicated by the following reactions:

$$LaCoO_3 + \tfrac{1}{2}Cl_2 \rightarrow LaOCl + \tfrac{1}{3}Co_3O_4 + \tfrac{1}{3}O_2 \quad (R1)$$

$$LaMnO_3 + \tfrac{1}{2}Cl_2 \rightarrow LaOCl + MnO_2 \quad (R2)$$

$$LaCoO_3 + \tfrac{1}{2}Cl_2 \rightarrow LaOCl + CoO + \tfrac{1}{2}O_2 \quad (R3)$$

$$LaMnO_3 + \tfrac{1}{2}Cl_2 \rightarrow LaOCl + MnO + \tfrac{1}{2}O_2 \quad (R4)$$

MnO_2 and Co_3O_4 are more stable at low temperatures whereas CoO and MnO are preferred at high temperatures. To calculate the free enthalpies of these reactions, the formation enthalpies of the different oxides, perovskites and LaOCl are required. It was possible to calculate the enthalpy of formation of $LaMnO_3$, $LaCoO_3$ and LaOCl versus temperature by using the results proposed by Yokokawa et al. [34] and the FACT software (facility for analysis of chemical thermodynamics) [35]. There is very good agreement between the calculated values that we obtained for the formation enthalpies ($kJ\,mol^{-1}$) of $LaCoO_3$ ($-1249.6 + 0.278T$, K) LaOCl ($-1013.2 + 0.174T$, K) and $LaMnO_3$ ($-1420.3 + 0.255T$, K) and the experimental values given by Yokokawa et al. [34]. The free enthalpy of the reactions R1 and R4 are represented in Fig. 12 as a function of temperature. The ΔG is negative for reactions R1 and R2 below 800°C, but the increase of the free enthalpy versus temperature is faster for R2 than for R1. At 300°C, ΔG is the same for reactions R1 and R2. The chlorination of $LaMnO_3$ and $LaCoO_3$ should be similar at this temperature. However, at 300°C, the conversion is low and thus the concentration of chlorine in the gas phase is low as well. It must also be taken into consideration that $LaMnO_3$ presents an oxygen overstoichiometry. Roosmalenand and Cordfunke

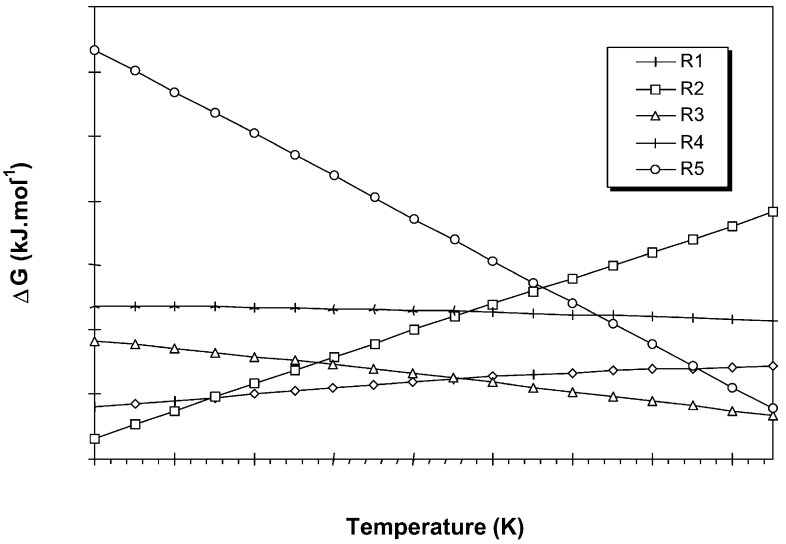

Fig. 12. Thermodynamic calculation of the stability of perovskites in the presence of gaseous chlorine.

[36] have calculated the enthalpies and entropies of formation of the $LaMnO_{3+\delta}$ overstoichiometric phase. Their results show that the overstoichiometric phase is thermodynamically favoured at low temperature:

$$LaMnO_3 + \tfrac{1}{2}\delta O_2 \rightarrow LaMnO_{3+\delta}\ \Delta G(T) = -380.2 + 0.266T\ (\mathrm{kJ\,mol^{-1}})$$

As a consequence, it was also possible to calculate the thermodynamic stability of $LaMnO_{3+\delta}$ in the presence of chlorine

$$LaMnO_{3+\delta} + \tfrac{1}{2}Cl_2 \rightarrow LaOCl + MnO_2 + \tfrac{1}{2}\delta O_2 \quad \text{(R5)}$$

The behaviour of the reaction R5 is different from that of reactions R2 and R4 (Fig. 12). Its free enthalpy is largely positive in the area of reaction temperature; it can therefore, be concluded that the formation of the overstoichiometric $LaMnO_{3+\delta}$ phase is the reason for the better stability of manganese perovskite compared to $LaCoO_3$ in the presence of chlorine. In the absence of oxygen in the feed, the framework oxygen takes part in the oxidation reaction. The manganese perovskite loses its oxygen overstoichiometry and its stability is destroyed according to reaction (R4).

5. Conclusion

$LaMO_3$ (M = Co, Mn) perovskites have been synthesised by a sol–gel-like method involving metallic propionate precursors. It has been shown by IRTF that the propionate species obtained starting from the metal or the nitrate salts are the same due to the elimination of the nitrate ligands as nitrous vapours. In both cases, bidentate metallic propionates are obtained. The use of nitrates presents the advantage of a faster solubilisation with respect to metals. On the contrary, the use of metallic chloride is not suitable because Cl^- is not easily exchanged by propionates. They remain in the gel and induce impurities in the final material or even avoid the perovskite formation like for cobalt where a mixture of LaOCl and Co_3O_4 was obtained after calcination. The results obtained during the perovskite preparation with chloride salts can be correlated with the ageing of the catalysts in the presence of chlorinated molecules. The $LaCoO_3$ perovskite is destroyed and LaOCl and Co_3O_4 are formed whereas $LaMnO_{3+\delta}$ is conserved. The better stability of the manganese perovskite in the presence of chlorine was attributed to a better thermodynamical stability of the oxygen overstoichiometric phase $LaMnO_{3+\delta}$ obtained after calcination. The destruction of the lanthanum cobalt perovskite leads to a deactivation of

the catalyst with CH_2Cl_2 but not with CCl_4. This difference is attributed to the different reaction pathways for the catalytic destruction of CH_2Cl_2 and CCl_4.

Acknowledgements

The authors are highly indebted to ADEME, The Region Alsace (FRANCE) and European Community (Contract No. EV5V-CT94-0530) for their financial support, and to L. Hilaire for discussions about XPS results.

References

[1] Anonymous, Inform. Chim. 387 (1997) 68.
[2] H. Sidebottom, J. Franklin, Pure Appl. Chem. 68 (1996) 1757.
[3] R.S. Stolarski, R.J. Cicerone, Can. J. Chem. 42 (1994) 1610.
[4] E. Nordally, J.R. Richmond, K.J. Drumm, in: S. Vigneron, J. Chaouki (Eds.), Characterisation and Control of Odours and VOC in the Process Industries, Elsevier, Amsterdam, Stud. Environ. Sci. 61 (1994) 459.
[5] H. Windawi, Z.C. Zhang, Catal. Today 30 (1996) 99.
[6] R.W. Van de Brink, P. Mulder, R. Louw, G. Sinquin, C. Petit, J.P. Hindermann, J. Catal. 180 (1998) 153.
[7] J.J. Spivey, Ind. Eng. Chem. Res. 26 (1987) 2165.
[8] R.M. Chintaware, H.L. Greene, J. Catal. 165 (1997) 12.
[9] G.J. Hutchings, C.S. Heneghan, I.D. Hudason, S.H. Taylor, Nature 384 (1996) 341.
[10] B. Chen, C. Bai, R. Cook, J. Wright, C. Wang, Catal. Today 30 (1996) 15.
[11] S.C. Petrosius, R.S. Drago, V. Young, G.C. Grunenwald, J. Am. Chem. Soc. 115 (1993) 6131.
[12] F. Solymosi, J. Rasko, E. Papp, A. Oszoko, T. Bansagi, Appl. Catal. A 131 (1995) 55.
[13] J.M.D. Tascon, G.L. Tejuca, J. Chem. Soc., Faraday Trans. 77 (1981) 591.
[14] G. Sinquin, C. Petit, J.P. Hindermann, A. Kiennemann, in: C.A.C. Sequeira, J.B. Moffat (Eds.), Faraday Discussion, Chemistry, Energy and Environment, 1998, p. 154.
[15] G. Sinquin, J.P. Hindermann, C. Petit, A. Kiennemann, Catal. Today 54 (1999) 107.
[16] G. Sinquin, C. Petit, S. Libs, J.P. Hindermann, A. Kiennemann, Appl. Catal. 27 (2000) 105.
[17] D. Kiessling, R. Scheider, P. Kraak, M. Haftendorn, G. Wendt, Appl. Catal. B 19 (1998) 143.
[18] J.L. Rehspringer, J.C. Bernier, Mat. Rec. Soc. Symp. Proc. 72 (1986) 67.
[19] A.C. Roger, C. Petit, A. Kiennemann, J. Catal. 167 (1997) 447.
[20] E. Spinner, P. Yang, P.T.T. Wong, H.H. Mantsch, Aust. J. Chem. 39 (1986) 475.
[21] P.F.R. Ewings, P.G. Harisson, J. Chem. Soc. Dalton (1975) 1717.
[22] C.D. Chandler, C. Roger, J.M. Hampden-Smith, Chem. Rev. 93 (1993) 1205.
[23] J.F. Ampion, D.A. Payne, H.K. Chae, J.K. Maurin, S.R. Wilson, Inorg. Chem. 30 (1991) 3244.
[24] A.C. Roger, Thesis, Université Louis Pasteur de Strasbourg, 1995.
[25] R.M. Lago, M.L.H. Green, S.C. Tsang, M. Odlyha, Appl. Catal. B 8 (1996) 107.
[26] M. Daturi, G. Busca, R.J. Willey, Chem. Mater. 7 (1995) 2115.
[27] Y. Okamoto, H. Nakano, T. Imanaka, S. Teranishi, Bull. Chem. Soc. Jpn. 48 (4) (1975) 1163.
[28] E.A. Lombardo, K. Tanaka, I. Toyoshima, J. Catal. 80 (1983) 340.
[29] H. Taguchi, A. Sugita, M. Nagao, J. Solid State Chem. 119 (1995) 164.
[30] R. Mariscal, J. Soria, M.A. Pena, J.L.G. Fierro, J. Catal. 147 (1994) 1482.
[31] J.H. Scofield, J. Electron Spectrosc. Relat. Phenom. 8 (1976) 129.
[32] K. Tabata, I. Matsumoto, S. Kohiki, J. Mater. Sci. 22 (1987) 1882.
[33] H. Taguchi, A. Sugita, M.J. Nagao, Y. Takeda, J. Solid State Chem. 116 (1995) 343.
[34] H. Yokokawa, S. Yamauchi, T. Matsumoto, Thermochim. Acta 245 (1994) 45.
[35] FACT Program. http:/www.crct.polymtl.ca/FACT/fact.htm.
[36] J.A.M. Roosmalenand, E.H.P. Cordfunke, J. Solid State Chem. 110 (1994) 109.